Noise-Enhanced Synchronization of Stochastic Magnetic Oscillators

N. Locatelli,[1,2] A. Mizrahi,[1,2] A. Accioly,[1,2,3] R. Matsumoto,[4] A. Fukushima,[4] H. Kubota,[4] S. Yuasa,[4] V. Cros,[1] L. G. Pereira,[3] D. Querlioz,[2] J.-V. Kim,[2] and J. Grollier[1,*]

[1]*Unité Mixte de Physique CNRS/Thales, 1 avenue A. Fresnel, Campus de l'Ecole Polytechnique, 91767 Palaiseau, France, and Université Paris-Sud, 91405 Orsay, France*

[2]*Institut d'Electronique Fondamentale, UMR CNRS 8622, Université Paris-Sud, 91405 Orsay, France*

[3]*Instituto de Física, Universidade Federal do Rio Grande do Sul, Porto Alegre 91501-970, Brazil*

[4]*National Institute of Advanced Industrial Science and Technology (AIST) 1-1-1 Umezono, Tsukuba, Ibaraki 305-8568, Japan*

(Received 16 May 2014; revised manuscript received 22 July 2014; published 16 September 2014)

We present an experimental study of phase locking in a stochastic magnetic oscillator. The system comprises a magnetic tunnel junction with a superparamagnetic free layer, whose magnetization dynamics is driven with spin torques through an external periodic driving current. We show that synchronization of this stochastic oscillator to the input current is possible for current densities below 3×10^6 A/cm^2, and occurs for input frequencies lower than the natural mean frequency of the stochastic oscillator. We show that such injection locking is robust and leads to a drastic reduction in the phase diffusion of the stochastic oscillator, despite the presence of a frequency mismatch between the oscillator and the excitation.

DOI: 10.1103/PhysRevApplied.2.034009

I. INTRODUCTION

Spin-torque-driven magnetic tunnel junctions (MTJs) exhibit a variety of dynamic behaviors, which, combined with their tiny size, CMOS compatibility, and endurance, make them promising candidates for a range of applications [1]. In particular, they are ideal model systems for the study of nonlinear dynamical phenomena. Under certain conditions, spin torques can lead to self-sustained precession of the magnetization and the junctions behave as nonlinear auto-oscillators, which can phase lock to an external signal [2–5], or even self-synchronize [6–8]. Phenomena related to the latter are currently the focus of much research, as it represents a promising means of improving the quality factor of such spin-torque nano-oscillators. However, the experimental demonstration of self-synchronization has been limited to a small number of spin-torque nano-oscillators ($N \leq 4$) [9,10].

Because of the small magnetic volume (or "active region") of such oscillators, the magnetization dynamics of these nano-objects is very sensitive to thermal fluctuations and other noise sources, resulting in a large phase noise that is detrimental to efficient phase locking and synchronization [11,12]. To make progress towards synchronization, one line of enquiry has involved studying modes that are less sensitive to noise, such as vortex gyration [13–15] or excitations in coupled bilayers [16,17]. Here, we instead pursue a different paradigm in which noise can be advantageous for improving coherence and facilitating synchronized states. This builds upon recent work in which spin-torque-driven magnetic tunnel junctions have been shown to exhibit stochastic resonance [18–21], i.e., a noise-enhanced sensitivity to very weak external stimuli [22]. Our work is focused on the *stochastic oscillator*, which involves a bistable state in which thermal fluctuations drive random transitions between the two states. Because such transitions involve a mean transition rate, an average frequency for the stochastic oscillator can be defined, and the presence of thermal fluctuations means that switching between the two states persists indefinitely without any external forcing.

Theoretical studies have shown that synchronization of such bistable stochastic oscillators is possible with an external harmonic excitation and occurs at an optimal noise level [23,24]. Experimentally, noise-enhanced synchronization has been mostly investigated in the context of biologic systems, thus requiring one to deal with extremely noisy and sparse data [25–27]. Very few in-depth studies deal with solid-state systems: these include Schmitt triggers [28,29], and lasers [30], which are mostly seen as toy systems to test the theoretical predictions. In this Letter, we demonstrate experimentally the noise-enhanced synchronization of a nanoscale physical system: the magnetic tunnel junction. In phase with the trend towards ultimate miniaturization, we exploit the increased impact of thermal fluctuations at reduced dimensions to synchronize the magnetic tunnel junction at very low energy cost and at room temperature, thus opening the path to real-world noise-leveraging applications.

*julie.grollier@thalesgroup.com

II. MAGNETIC TUNNEL JUNCTION AS A STOCHASTIC OSCILLATOR

Our system is a superparamagnetic tunnel junction: at zero or small bias, the free-layer magnetization constantly fluctuates between the parallel (P) and antiparallel (AP) states under thermal fluctuations. This system is particularly interesting for two main reasons. First, the energy barrier between the P and AP states is low, which allows the magnetic configuration to be manipulated with spin torques at very small current densities. Second, the junction naturally behaves as a stochastic oscillator as described above. We show using time-resolved experiments that, despite its stochastic nature, phase synchronization of the superparamagnetic tunnel junction can be achieved by using low densities for the ac excitation current ($< 3 \times 10^6$ A/cm^2) compared to those usually required for spin-torque nano-oscillators [2–5]. By investigating the phase-diffusion processes at stake we demonstrate the existence of a critical frequency under which the noisy system is able to lock to the excitation.

The stochastic oscillator is a magnetic tunnel junction with an elliptical cross-section of 60×180 nm^2, composed of a reference synthetic-antiferromagnetic (SAF) trilayer of CoFe (2.5 nm)/Ru (0.85 nm)/CoFeB (3 nm), an MgO tunnel barrier (1.05 nm), and a CoFeTiB (2 nm) free layer [Fig. 1(a)]. The free-layer magnetization is bistable, where the energy barrier separating the two states is designed to be sufficiently low such that thermally induced switching of the free-layer magnetization from one state to the other occurs at room temperature [Fig. 1(b)]. The MTJ is then said to be superparamagnetic (SP) and oscillates stochastically between the P and AP states, generating a telegraph resistance signal due to the large tunneling magnetoresistance (TMR) of the junction [Fig. 1(c)]. Under constant bias, the dwell times in each state follow a Poisson distribution [Fig. 1(d)] [31]. For instance, we measure at low currents ($I_{dc} = 100$ μA) mean dwell times of $\langle \tau_{AP} \rangle = 8.5$ ms in the high-resistance AP state and $\langle \tau_P \rangle = 10.1$ ms in the low-resistance P state. In this "free-running" regime, the junction behaves as a stochastic oscillator and can be characterized by its mean frequency, defined by $\langle F \rangle = 1/(\langle \tau_P \rangle + \langle \tau_{AP} \rangle)$, which corresponds to $\langle F \rangle = 53.8$ Hz here. As illustrated in Fig. 1(b), depending on the sign of the injected current, the spin torque will favor one state over the other, such that $\langle \tau_{P,AP} \rangle = \tau_0 \exp[\Delta E(1 \mp I/I_C)/(k_B T)]$, where τ_0 is the attempt time, k_B is the Boltzmann constant, T is the temperature, ΔE is the energy barrier between P and AP states at zero bias, and I_C is the critical switching current at zero temperature [31,32]. In our convention, a positive current tends to stabilize the (AP) magnetization state. In the following, all measurements are performed at zero effective field, in other words with an applied external field of -37 Oe compensating the stray field from the SAF, so that both P and AP states show equal stabilities at zero current. From the experimental value of the zero-current dwell times (about 10 ms in each state), and assuming an attempt time τ_0 of 1 ns [31], we can derive that the ratio of the energy barrier to the thermal energy $\Delta E/(k_B T)$ is close to 16, a small value in agreement with the superparamagnetic nature of our junction. Fitting the resistance versus current curve in Fig. 1(e) with $R = R_P + \Delta R/\{1 + \exp[2\Delta E/(k_B T) I/I_c]\}$ allows us to derive the zero-temperature critical current of our junction: $I_C = 1.5$ mA, which corresponds to a critical current density of 1.8×10^7 A/cm^2.

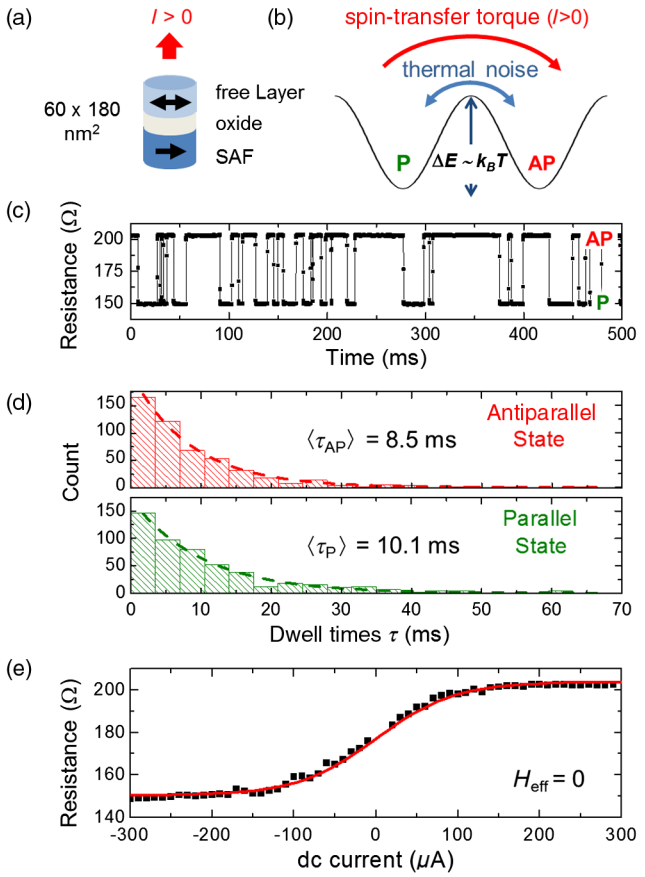

FIG. 1. (a) Schematic of the magnetic tunnel junction stack. (b) Schematic of double-well energy landscape for the free-layer magnetization, that can hop between the P and AP states with the assistance of thermal fluctuations and spin torque. (c) Sample of the telegraphic temporal resistance evolution generated by the MTJ, measured at room temperature under a $I_{dc} = 100$ μA current and an applied field of -30 Oe which combined with the stray field from the SAF favors the P state. (d) Associated dwell-time distributions for P and AP states, fitted by an exponential envelope corresponding to a Poissonian distribution. (e) Resistance versus dc current curve obtained at zero effective field, i.e., with an applied field of -37 Oe compensating the stray field of the synthetic antiferromagnet.

III. EXPERIMENTAL STUDY

A. Behavior under weak current excitation

We study the response of the SP MTJ to a weak oscillating excitation current. Under the zero effective field,

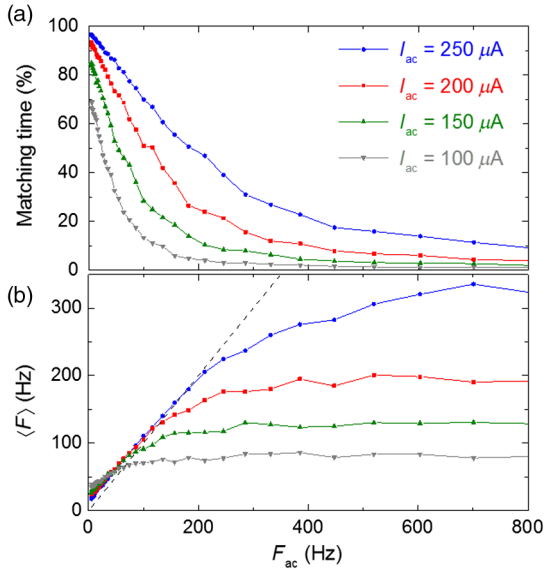

FIG. 2. MTJ response to different current amplitudes $I_{ac} = 250$, 200, 150, and 100 μA. (a) Matching time between the resistance response and the excitation signal. (b) Average oscillation frequency of the resistance response $\langle F \rangle$ versus excitation frequency F_{ac}. The dashed line corresponds to a match between response and excitation frequencies.

we inject a square-wave periodic current of different amplitudes well below the critical current of our junction, $I_{ac} = 250$, 200, 150, and 100 μA, and frequencies between 5 Hz and 2 kHz, and we monitor the voltage across the junction with an oscilloscope. For each ac-current amplitude I_{ac} and frequency F_{ac} considered, 10 traces of 2 s in duration are recorded in order to obtain sufficient statistics on the response of the stochastic device. By analyzing the voltage data, we construct the time evolution of the free-layer magnetization and examine how it is influenced by the different parameters of the input ac current.

A first method to quantify the correlation between the stochastic oscillator and the excitation source involves the percentage of time during which the two signals are in phase, which we denote as the "matching time." Figure 2(a) shows that this matching time increases monotonously as the excitation frequency F_{ac} decreases. This feature is characteristic of stochastic resonance [22] and has already been observed in other studies [18–20]. When the driving frequency is large compared to the natural oscillation rate of the stochastic oscillator, the latter does not respond to the input signal, and the matching time is small. By lowering the input frequency, the ability of the oscillator to adjust to the external forcing increases, and the matching time also increases accordingly. As Fig. 2(a) shows, the matching time also increases with increasing amplitude of the ac current, reaching values of 96.8% at 5 Hz and $I_{ac} = 250$ μA.

However, the matching time does not provide any information regarding the influence that the excitation current has on the frequency of the stochastic oscillator. To investigate this point, we also examined the evolution of the mean oscillation frequency $\langle F \rangle$ as a function of the frequency of the excitation current F_{ac} [Fig. 2(b)]. When the frequency of the input signal is too large for the magnetization to follow, the mean frequency of the stochastic oscillator plateaus to a constant value that is determined by the amplitude of the ac current. When the excitation frequency is reduced, on the other hand, we observe a clear pulling of the mean frequency of the stochastic oscillator toward the excitation frequency. This pulling effect becomes more efficient as the amplitude of the excitation increases. However, as Fig. 2(b) shows, the mean frequency of the stochastic oscillator deviates from the frequency of the input signal (dashed line) at low frequencies at which the matching time percentage increases.

B. Stochastic resonance and synchronization

In order to get a better insight into this effect, we examine the time traces of the SP MTJ response for different frequencies of the excitation current. The square-wave current of amplitude $I_{ac} = 250$ μA and the temporal resistance evolution of the MTJ are shown in Figs. 3(a) and 3(b), respectively. We also reconstruct the piecewise linear phases [24] associated with both the current (φ_e) and magnetization (φ_s) oscillations [Fig. 3(c)] and extracted the dwell-time distributions for both P and AP states [Fig. 3(d)].

Let us first consider the case of a high excitation frequency $F_{ac} = 450$ Hz compared to the natural frequency $\langle F \rangle$ of the oscillator (Fig. 3, left column). As the resistance time trace shows, the magnetization switching is largely correlated with the reversals of the current polarity [Figs. 3(a) and 3(b)]. A direct consequence is that the dwell times no longer follow a Poisson distribution, as observed when a constant current is applied, but rather exhibit peaks around $(n + 1/2)T_{ac}$, where T_{ac} is the period of the excitation [Fig. 3(c)]. Such correlations can be explained as follows. A dwell time close to $T_{ac}/2$ means that two consecutive ac-current polarity reversals both induce a magnetization reversal. If the system does not follow a polarity reversal, it has to wait for one more period for the next reversal ($\tau \approx 3T_{ac}/2$), or two more periods ($\tau \approx 5T_{ac}/2$), and so on. Nevertheless, the stochastic nature of the switching still manifests itself in the Poisson-like decay in the amplitude of the peaks in the dwell-time distribution as τ increases. While the MTJ responds resonantly under the influence of the excitation, due to the phenomenon of stochastic resonance, synchronization to the external signal is not achieved. The mean oscillation frequency of the stochastic oscillator $\langle F \rangle = 282$ Hz [Fig. 2(b)] remains significantly lower than the excitation frequency F_{ac} and the matching time between the two signals is low at 17.4% [Fig. 2(a)]. This can also be seen in

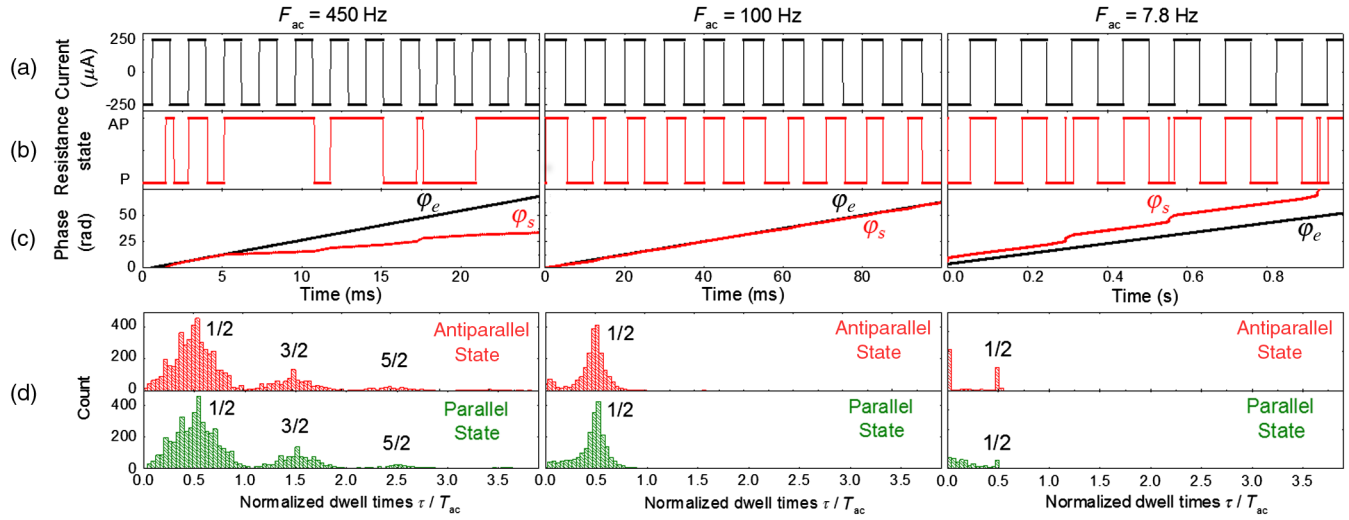

FIG. 3. SP MTJ response to square-wave current excitations with 250 μA amplitude and frequencies $F_{ac} = 450$ Hz (left), $F_{ac} = 100$ Hz (center), $F_{ac} = 7.8$ Hz (right). Sample of the temporal evolution of (a) the current through the MTJ, (b) its resistance response, and (c) the piecewise linear reconstructed phase for the current (φ_e, black) and for the resistance (φ_s, red). (d) Associated dwell-time distributions for both high (AP) and low (P) resistance states.

the piecewise linear phase evolution, where the phase of the stochastic oscillator increases more slowly than the phase of the input square wave, with no visible correlation between the two [Fig. 3(c)].

As the excitation frequency is reduced to $F_{ac} = 100$ Hz, the response of the system changes and the stochastic nature of the oscillator becomes less apparent (Fig. 3, center column). As the resistance time traces show, the magnetization switches with each reversal of the current polarity and the dwell-time distributions exhibit only one peak around $T_{ac}/2$. In addition, we note almost no occurrence during the 20-sec measurement of a dwell time superior to T_{ac}, which would indicate one missed oscillation or phase slip. Furthermore, the reconstructed phase of the stochastic oscillator exhibits a quasilinear variation and follows closely the phase of the input signal. As such, the stochastic behavior is considerably reduced and is observed only as small, bounded fluctuations of the piecewise linear phase shift $\Delta\varphi$ around zero. A near-perfect phase synchronization is therefore achieved during this time interval for low current densities, since 250 μA in our junctions corresponds to a density below 3×10^6 A/cm^2. The mean frequency of the stochastic oscillator is measured to be $\langle F \rangle = 111$ Hz [Fig. 2(b)] and the matching percentage has increased to 70.0% [Fig. 2(a)].

As the excitation frequency is further reduced to $F_{ac} = 7.8$ Hz, we observe the appearance of a large number of "glitches" in the magnetization switching (Fig. 3, right column). Since the current remains in each polarity for a long time compared to the natural dwell times, the probability of thermally driven back-and-forth switching of the magnetization increases, which gives rise to the observed glitches. These events occur over a short time scale compared to the period of the input square-wave current and appear as localized 2π jumps in the phase of the stochastic oscillator. Outside of these glitches, the magnetization is seen to switch with each reversal of the current polarity, which results in a quasilinear variation of the stochastic oscillator phase. While the matching percentage reaches a very high value of 95.9%, the presence of the glitches leads to an increase in the mean frequency of the stochastic oscillator oscillation, $\langle F \rangle = 20.1$ Hz, which is significantly larger than the excitation frequency.

C. Phase diffusion

The broad features of the variation of the dwell-time distribution with the frequency of the input forcing signal described above are consistent with previous theoretical and experimental work on periodically forced bistable systems. However, while phase locking of stochastic oscillators has been studied previously, the existence of glitches in the synchronized state and their role in frequency mismatches have not been considered theoretically to the best of our knowledge [23,24]. In fact, these glitches and the associated phase jumps are very similar in nature to the thermally induced phase slips that can be observed when noisy oscillators are phase locked. Quantifying this phenomenon is therefore crucial for applications. To do so, we analyze the phase evolution of the stochastic magnetic oscillator as a one-dimensional random walk. Using the measured time traces, we can derive the diffusion constant for the phase [23,24],

$$D_{\text{eff}} = \frac{1}{2}\frac{d}{dt}[\langle \varphi_{s,i}{}^2(t)\rangle_i - \langle \varphi_{s,i}(t)\rangle_i^2], \qquad (1)$$

which quantifies the randomness of the evolution of magnetization oscillations, and $D_{\text{eff}} = 0$ would correspond

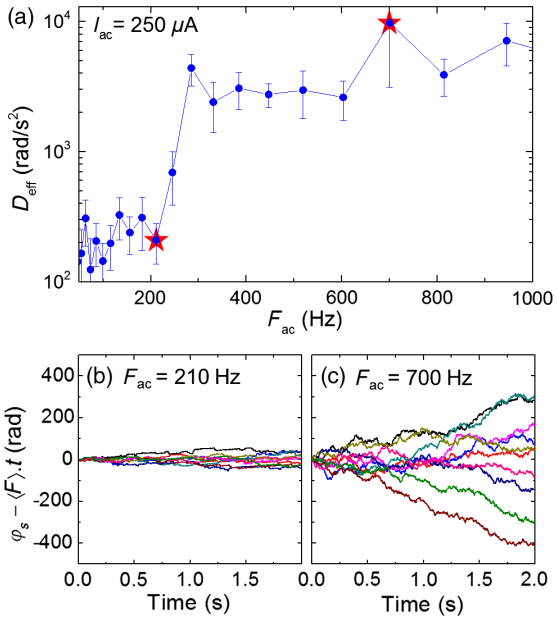

FIG. 4. (a) Effective diffusion constant D_{eff} as a function of the input excitation frequency F_{ac} for a current amplitude $I_{\text{ac}} = 250\ \mu$A. Ten time traces of the stochastic oscillator phase for input frequencies of (b) 210 Hz and (c) 700 Hz, indicated by the red stars in (a). The linear variation corresponding to the average frequency is subtracted for clarity.

to a deterministic (e.g., perfectly harmonic) behavior of the oscillator. Here, the index $i \in [1, \ldots, 10]$ corresponds to the measurement number. The evolution of the diffusion coefficient versus excitation frequency at constant current amplitude is shown in Fig. 4(a) for $I_{\text{ac}} = 250\ \mu$A. We note a drastic transition from the random to the synchronized regime starting at a critical frequency $F_C \approx 300$ Hz, which is very close to the natural frequency of the stochastic oscillator for this input current amplitude [320 Hz, as shown in Fig. 2(b)]. The system indeed switches from a high excitation frequency regime where the diffusion constant is large, corresponding to the free-running stochastic oscillator, to a regime at low excitation frequencies where the oscillator is entrained by the ac-current input signal. This result shows that despite the glitches and the difference between the average oscillation rate and the excitation frequency, the stochastic oscillator falls into a synchronized regime in which it is phase locked to the excitation. To illustrate the difference in the dispersion below and above the critical frequency, we present in Figs. 4(b) and 4(c) the 10 $\varphi_s(t)$ measurements for $F_{\text{ac}} =$ 210 Hz and $F_{\text{ac}} = 700$ Hz, respectively, on the same scale. We can clearly see that for $F_{\text{ac}} > F_C$ the dispersion between oscillators is very high, while the dispersion is strongly suppressed by external excitation for $F_{\text{ac}} < F_C$. The nonvanishing D_{eff} in the synchronized regime represents the remaining stochastic behavior associated with the random occurrence of glitches and thermal fluctuations.

IV. CONCLUSION

In conclusion, we demonstrate that a stochastic magnetic oscillator can phase lock to an input signal with a frequency lower than the natural frequency of the oscillator. While the synchronization is not perfect due to unavoidable phase slips, it occurs for forcing current densities of the order of 3×10^6 A/cm^2, one order of magnitude below the critical values required for deterministic switching at zero temperature. We therefore leverage an effect that appears only at nanoscale dimensions: superparamagnetism, and exploit the effect of thermal fluctuations for synchronization instead of suffering from this noise. Given that nanoscale magnetic tunnel junctions, building blocks of magnetic memories, are a CMOS-compatible, mature technology, our demonstration of their stochastic synchronization finally opens the path towards noise-leveraging applications. In particular, this system is extremely promising for applications where low energy is crucial, such as bioinspired associative memories based on coupled spin-torque nano-oscillator networks [33].

ACKNOWLEDGMENTS

The authors acknowledge financial support from the FET-OPEN Bambi project No. 618024. A. A. acknowledges financial support from the Brazilian Agency National Council for Scientific and Technological Development (CNPq, Project No. 245555/2012-9), and A. M. from the Ile-de-France regional government through the DIM nano-K program.

[1] N. Locatelli, V. Cros, and J. Grollier, Spin-torque building blocks, Nat. Mater. **13**, 11 (2014).
[2] W. H. Rippard, M. R. Pufall, S. Kaka, T. J. Silva, S. E. Russek, and J. A. Katine, Injection locking and phase control of spin transfer nano-oscillators, Phys. Rev. Lett. **95**, 067203 (2005).
[3] B. Georges, J. Grollier, M. Darques, V. Cros, C. Deranlot, B. Marcilhac, G. Faini, and A. Fert, Coupling efficiency for phase locking of a spin transfer nano-oscillator to a microwave current, Phys. Rev. Lett. **101**, 017201 (2008).
[4] Sergei Urazhdin, Phillip Tabor, Vasil Tiberkevich, and Andrei Slavin, Fractional synchronization of spin-torque nano-oscillators, Phys. Rev. Lett. **105**, 104101 (2010).
[5] A. Dussaux, A. V. Khvalkovskiy, J. Grollier, V. Cros, A. Fukushima, M. Konoto, H. Kubota, K. Yakushiji, S. Yuasa, K. Ando, and A. Fert, Phase locking of vortex based spin transfer oscillators to a microwave current, Appl. Phys. Lett. **98**, 132506 (2011).
[6] Shehzaad Kaka, Matthew R. Pufall, William H. Rippard, Thomas J. Silva, Stephen E. Russek, and Jordan A. Katine, Mutual phase locking of microwave spin torque nano-oscillators, Nature (London) **437**, 389 (2005).
[7] F. B. Mancoff, N. D. Rizzo, B. N. Engel, and S. Tehrani, Phase-locking in double-point-contact spin-transfer devices, Nature (London) **437**, 393 (2005).

[8] J. Grollier, V. Cros, and A. Fert, Synchronization of spin-transfer oscillators driven by stimulated microwave currents, Phys. Rev. B **73**, 060409 (2006).

[9] A. Ruotolo, V. Cros, B. Georges, A. Dussaux, J. Grollier, C. Deranlot, R. Guillemet, K. Bouzehouane, S. Fusil, and A. Fert, Phase-locking of magnetic vortices mediated by antivortices, Nat. Nanotechnol. **4**, 528 (2009).

[10] S. Sani, J. Persson, S. M. Mohseni, Ye Pogoryelov, P. K. Muduli, A. Eklund, G. Malm, M. Käll, A. Dmitriev, and J. Åkerman, Mutually synchronized bottom-up multi-nanocontact spin-torque oscillators, Nat. Commun. **4**, 2731 (2013).

[11] M. Quinsat, D. Gusakova, J. F. Sierra, J. P. Michel, D. Houssameddine, B. Delaet, M.-C. Cyrille, U. Ebels, B. Dieny, L. D. Buda-Prejbeanu, J. A. Katine, D. Mauri, A. Zeltser, M. Prigent, J.-C. Nallatamby, and R. Sommet, Amplitude and phase noise of magnetic tunnel junction oscillators, Appl. Phys. Lett. **97**, 182507 (2010).

[12] Eva Grimaldi, Antoine Dussaux, Paolo Bortolotti, Julie Grollier, Grégoire Pillet, Akio Fukushima, Hitoshi Kubota, Kay Yakushiji, Shinji Yuasa, and Vincent Cros, Response to noise of a vortex based spin transfer nano-oscillator, Phys. Rev. B **89**, 104404 (2014).

[13] Q. Mistral, M. van Kampen, G. Hrkac, Joo-Von Kim, T. Devolder, P. Crozat, C. Chappert, L. Lagae, and T. Schrefl, Current-driven vortex oscillations in metallic nanocontacts, Phys. Rev. Lett. **100**, 257201 (2008).

[14] V. S. Pribiag, I. N. Krivorotov, G. D. Fuchs, P. M. Braganca, O. Ozatay, J. C. Sankey, D. C. Ralph, and R. A. Buhrman, Magnetic vortex oscillator driven by d.c. spin-polarized current, Nat. Phys. **3**, 498 (2007).

[15] A. Dussaux, B. Georges, J. Grollier, V. Cros, A. V. Khvalkovskiy, A. Fukushima, M. Konoto, H. Kubota, K. Yakushiji, S. Yuasa, K. A. Zvezdin, K. Ando, and A. Fert, Large microwave generation from current-driven magnetic vortex oscillators in magnetic tunnel junctions, Nat. Commun. **1**, 1 (2010).

[16] N. Locatelli, V. V. Naletov, J. Grollier, G. de Loubens, V. Cros, C. Deranlot, C. Ulysse, G. Faini, O. Klein, and A. Fert, Dynamics of two coupled vortices in a spin valve nanopillar excited by spin transfer torque, Appl. Phys. Lett. **98**, 062501 (2011).

[17] D. Gusakova, M. Quinsat, J. F. Sierra, U. Ebels, B. Dieny, L. D. Buda-Prejbeanu, M.-C. Cyrille, V. Tiberkevich, and A. N. Slavin, Linewidth reduction in a spin-torque nano-oscillator caused by non-conservative current-induced coupling between magnetic layers, Appl. Phys. Lett. **99**, 052501 (2011).

[18] X. Cheng, C. T. Boone, J. Zhu, and I. N. Krivorotov, Nonadiabatic stochastic resonance of a nanomagnet excited by spin torque, Phys. Rev. Lett. **105**, 047202 (2010).

[19] X. Cheng, J. A. Katine, G. E. Rowlands, and I. N. Krivorotov, Nonlinear ferromagnetic resonance induced by spin torque in nanoscale magnetic tunnel junctions, Appl. Phys. Lett. **103**, 082402 (2013).

[20] G. Finocchio, I. N. Krivorotov, X. Cheng, L. Torres, and B. Azzerboni, Micromagnetic understanding of stochastic resonance driven by spin-transfer-torque, Phys. Rev. B **83**, 134402 (2011).

[21] M. d'Aquino, C. Serpico, R. Bonin, G. Bertotti, and I. D. Mayergoyz, Stochastic resonance in noise-induced transitions between self-oscillations and equilibria in spin-valve nanomagnets, Phys. Rev. B **84**, 214415 (2011).

[22] Luca Gammaitoni, Peter Hänggi, Peter Jung, and Fabio Marchesoni, Stochastic resonance, Rev. Mod. Phys. **70**, 223 (1998).

[23] Alexander Neiman, Alexander Silchenko, Vadim Anishchenko, and Lutz Schimansky-Geier, Stochastic resonance: Noise-enhanced phase coherence, Phys. Rev. E **58**, 7118 (1998).

[24] Jan A. Freund, Lutz Schimansky-Geier, and Peter Hänggi, Frequency and phase synchronization in stochastic systems, Chaos **13**, 225 (2003).

[25] S. Bahar, A. Neiman, L. A. Wilkens, and F. Moss, Phase synchronization and stochastic resonance effects in the crayfish caudal photoreceptor, Phys. Rev. E **65**, 050901(R) (2002).

[26] T. Mori and S. Kai, Noise-induced entrainment and stochastic resonance in human brain waves, Phys. Rev. Lett. **88**, 218101 (2002).

[27] A. Samardak, A. Nogaret, N. B. Janson, A. G. Balanov, I. Farrer, and D. A. Ritchie, Noise-controlled signal transmission in a multithread semiconductor neuron, Phys. Rev. Lett. **102**, 226802 (2009).

[28] B. Shulgin, A. Neiman, and V. Anishchenko, Mean switching frequency locking in stochastic bistable systems driven by a periodic force, Phys. Rev. Lett. **75**, 4157 (1995).

[29] I. A. Khovanov and P. V. E. McClintock, Synchronization of stochastic bistable systems by biperiodic signals, Phys. Rev. E **76**, 031122 (2007).

[30] S. Barbay, G. Giacomelli, S. Lepri, and A. Zavatta, Experimental study of noise-induced phase synchronization in vertical-cavity lasers, Phys. Rev. E **68**, 020101(R) (2003).

[31] William Rippard, Ranko Heindl, Matthew Pufall, Stephen Russek, and Anthony Kos, Thermal relaxation rates of magnetic nanoparticles in the presence of magnetic fields and spin-transfer effects, Phys. Rev. B **84**, 064439 (2011).

[32] Z. Li and S. Zhang, Thermally assisted magnetization reversal in the presence of a spin-transfer torque, Phys. Rev. B **69**, 134416 (2004).

[33] G. Csaba, M. Pufall, D. E. Nikonov, G. I. Bourianoff, A. Horvath, T. Roska, and W. Porod, Spin torque oscillator models for applications in associative memories, in *Proceedings of the 13th International Cellular Nanoscale Networks and Their Applications (CNNA) Workshop, 2012* (IEEE, Turin, 2012), pp. 1 and 2.